Cancer Letters 447 (2019) 154–163

Contents lists available at ScienceDirect

Cancer Letters

journal homepage: www.elsevier.com/locate/canlet

Original Articles

ROS-generating oxidase NOX1 promotes the self-renewal activity of CD133 + thyroid cancer cells through activation of the Akt signaling

Cong Wang, Zhenglin Wang, Wei Liu, Zhilong Ai*

Department of General Surgery, Zhongshan Hospital, Fudan University, Shanghai, 200032, China

ARTICLE INFO

Keywords:
Cancer stem cells
Tumorigenesis
STAT3
Gene expression

ABSTRACT

Thyroid cancer results from unregulated expansion of a self-renewing tumor-initiating cell population. The regulatory pathways essential for sustaining the self-renewal of tumor-initiating cells remain largely unknown. Reactive oxygen species (ROS) play a vital role in tumor initiation and progression. In the present study, we found that the level of ROS was higher in CD133 + thyroid cancer cells than in CD133- thyroid cancer cells. The transcriptional level of ROS-generating oxidase NADPH oxidase 1 (NOX1) is high in CD133 + thyroid cancer cells. Activation of STAT3 through phosphorylation is responsible for high activation of NOX1 transcription in CD133 + thyroid cancer cells. Knock down of NOX1 obviously reduced the level of ROS and inhibited the self-renewal activity and tumorigenicity of CD133 + thyroid cancer cells. Furthermore, knock down of NOX1 reduced the activity of PI3K/Akt pathway. Overexpression of active form of Akt rescued the negative effect of NOX1 knockdown on the self-renewal capability of CD133 + thyroid cancer cells. Together, NOX1 promotes the self-renewal property of CD133 + thyroid cancer cells at least partly through activation of the Akt signaling.

1. Introduction

Thyroid cancer is the most common type of endocrine cancer. Its incidence is growing rapidly over the last 20 years [1]. Understanding the mechanisms underlying thyroid cancer initiation and progression will aid in treating thyroid cancer [2]. Cancer stem cells are responsible for the initiation, propagation, and recurrence of tumors [3,4]. For thyroid cancer, CD133 is a marker of thyroid cancer stem cells [5]. CD133 + thyroid cancer cells exhibited stem-cell-like features such as self-renewal and differential potential [6]. However, the pathways sustaining the self-renewal of thyroid cancer stem cells remain largely unknown.

Cancer cells tend to have persistently high levels of reactive oxygen species (ROS) [7,8]. ROS play a vital role during cancer initiation and progression [9]. An increase in intracellular ROS levels activates tumorigenesis-associated pathways, including the MAPK and PI3K/Akt pathways [10]. However, the contribution of ROS to thyroid cancer stem cells self-renewal remains largely unknown.

In the present study, we found that the level of ROS was higher in CD133 + thyroid cancer cells than in CD133-thyroid cancer cells. The transcriptional level of ROS-generating oxidase NADPH oxidase 1 (NOX1) is high in CD133 + thyroid cancer cells. Knock down of NOX1 reduced the level of ROS and inhibited the self-renewal activity and tumorigenicity of CD133 + thyroid cancer cells. Furthermore, knock down of NOX1 reduced the activity of PI3K/Akt pathway. Overexpression of active form of Akt rescued the negative effect of NOX1 knockdown on the self-renewal capability of CD133 + thyroid cancer cells. Altogether, NOX1 promotes the self-renewal property of CD133 + thyroid cancer cells at least partly through activation of the Akt signaling.

2. Materials and methods

2.1. Cell lines and cell culture

Thyroid cancer cell lines C643 and 8305C were purchased from Cell Bank affiliated to China Academy of Science and were cultured in Dulbecco's modified Eagle's medium supplemented with 10% fetal bovine serum containing 100 U/ml penicillin and 50 μg/ml streptomycin. Cells were cultured at 37 °C in a humidified CO_2 incubator (5% CO2, 95% air).

The sorted CD133 + cells isolated from xenograft formed from thyroid cancer cells were cultured in the DMEM/F12 media supplemented with B27 lacking vitamin A (Invitrogen), 2 μg/ml heparin

Abbreviations: ROS, reactive oxygen species; shRNA, short hairpin RNA; HRP, horseradish peroxidase; GAPDH, glyceraldehyde-3-phosphate dehydrogenase; LV, lentiviral; NOX1, NADPH oxidase 1; PVDF, polyvinylidene difluoride; CSC, cancer stem cell; BSO, L-buthionine sulfoximine; NAC, N-acetyl-L-cysteine

* Corresponding author.
E-mail address: azlong_fudan@163.com (Z. Ai).

https://doi.org/10.1016/j.canlet.2019.01.028
Received 3 October 2018; Received in revised form 31 December 2018; Accepted 22 January 2019

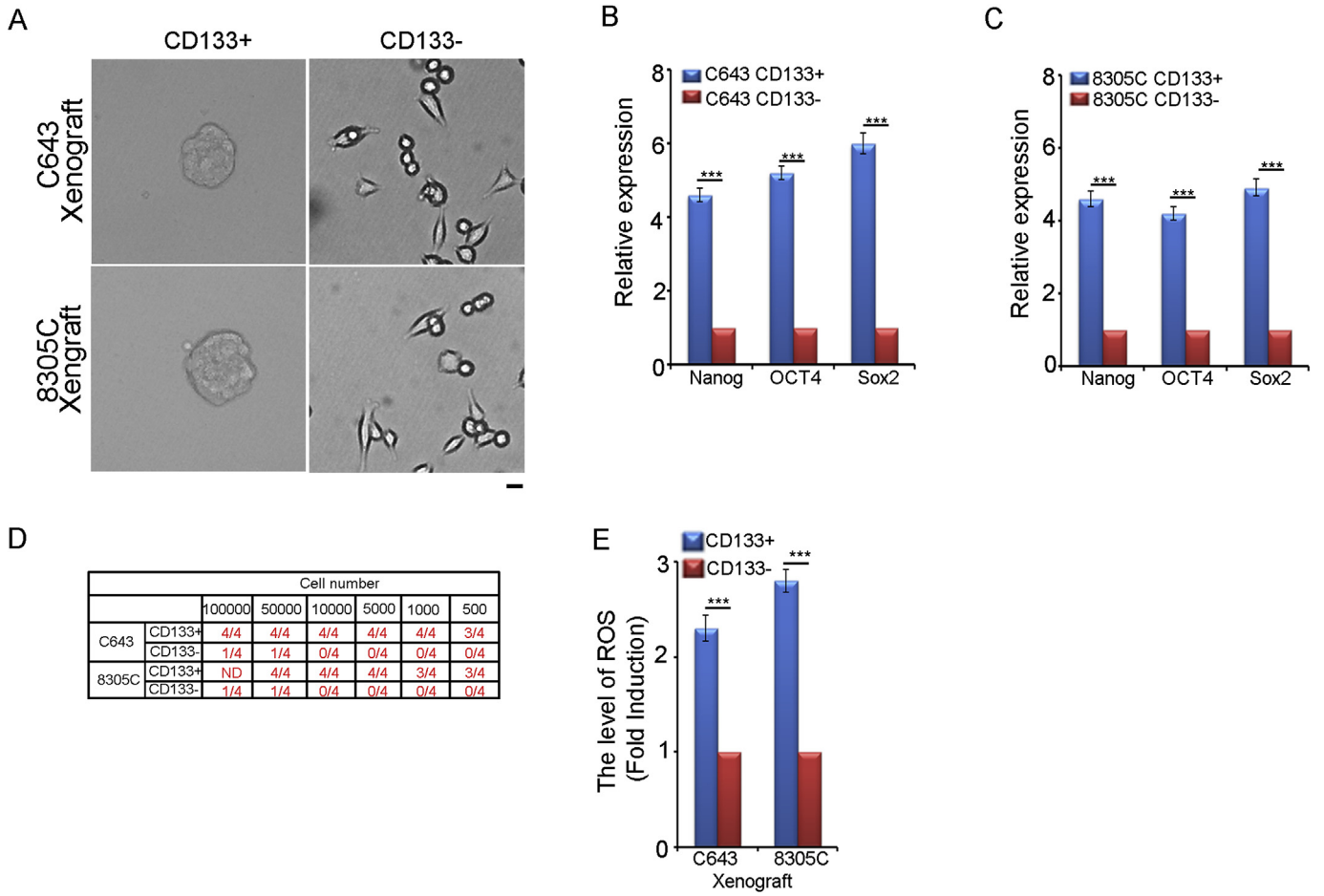

		Cell number					
		100000	50000	10000	5000	1000	500
C643	CD133+	4/4	4/4	4/4	4/4	4/4	3/4
	CD133-	1/4	1/4	0/4	0/4	0/4	0/4
8305C	CD133+	ND	4/4	4/4	4/4	3/4	3/4
	CD133-	1/4	1/4	0/4	0/4	0/4	0/4

Fig. 1. The level of ROS is higher in CD133 + thyroid cancer cells. (A) Representative image of spheres from CD133 + cells isolated from xenograft formed from thyroid cancer cells (C643 or 8305C). Scale bar represents 10 μM. (B and C) QPCR analysis was performed for stem cell-associated genes in CD133 + cells versus CD133- cells isolated from C643 xenograft (B) or 8305C xenograft (C). CD133- cells were defined as 1, and the relative expression of each gene in CD133 + cells was expressed as the fold difference over CD133-cells. (D) An in vivo limiting dilution tumor formation assay (employing 100,000, 50,000, 10,000, 5,000, 1000 or 500 cells per mouse) was performed to compare the tumor-initiating capacity of CD133 + cells or CD133- cells isolated from C643 xenograft or 8305C xenograft. Mice were sacrificed when they were moribund or 180 days after implantation. Tumor formation was determined by histology. (E) The level of ROS in CD133 + cells and CD133- cells were analyzed by FACS. The level of ROS in CD133- cells were defined as 1 (calibrator). Results are expressed as mean ± SEM from three separate experiments; ***$p < 0.001$.

(Sigma), 20 ng/ml EGF (Chemicon) and 10 ng/ml FGF-2 (Chemicon) for a short period before treatment and analysis. CD133- tumor cells were plated in DMEM with 10% fetal bovine serum for at least 12 h to permit cells survival. Prior to performing experiments with CD133- cells, DMEM with 10% fetal bovine serum was replaced with supplemented DMEM/F12 media in order for experiments to be performed in identical media. Cell transient transfection with plasmids or siRNA was performed with Lipofectamine 2000 (Invitrogen) according to the manufacturer's instructions. Cells were harvested 48-72 h after transfection.

2.2. Lentiviral shRNAs

Briefly, using calcium phosphate transfection, 293T cells were co-transfected with lentiviral vector expressing LacZ shRNA or NOX1 shRNA, and the packaging vectors RRE, REV and RSVG. Two days later, the supernatants were collected and concentrated. Cells were transduced by using lentivirus with polybrene (Sigma; 8 μg/ml). Following infection for 48 h, cells were selected with 2.0 mg/ml G418 (Sigma). Knockdown efficiencies were confirmed via western blotting.

2.3. Sphere formation assay

CD133 + thyroid cancer cells were cultured in serum-free DMEM/F12 media (Invitrogen), supplemented with 20 ng/ml EGF (Chemicon), 10 ng/ml human recombinant bFGF Chemicon), and B27 (Invitrogen). Cells were cultured in suspension in 96-well plates at different density. After 10 days, the number of spheres with diameter > 50 μM was quantified.

2.4. Western blot

Equal amounts of cell lysate were resolved by SDS-PAGE, transferred to polyvinylidene difluoride (PVDF) membranes (Roche). Blocking was performed for 60 min with 5% nonfat dry milk or %1 BSA in TBST. Blotting was performed with primary antibodies for 12–16 h at 4 °C. Primary antibodies included: rabbit polyclonal anti-NOX1 antibody (Abcam), rabbit monoclonal anti-GAPDH antibody (Cell signaling), rabbit monoclonal anti-phospho-Akt (Thr308) antibody (Cell signaling), rabbit polyclonal anti-Akt antibody (Cell signaling), and mouse monoclonal anti-phospho-STAT3 antibody (BD Biosciences). After extensive washing with TBST, the membranes were incubate for 1.5–2 h at room temperature with HRP-conjugated goat anti-rabbit antibody (Santa Cruz Biotechnology), and signal was detected by

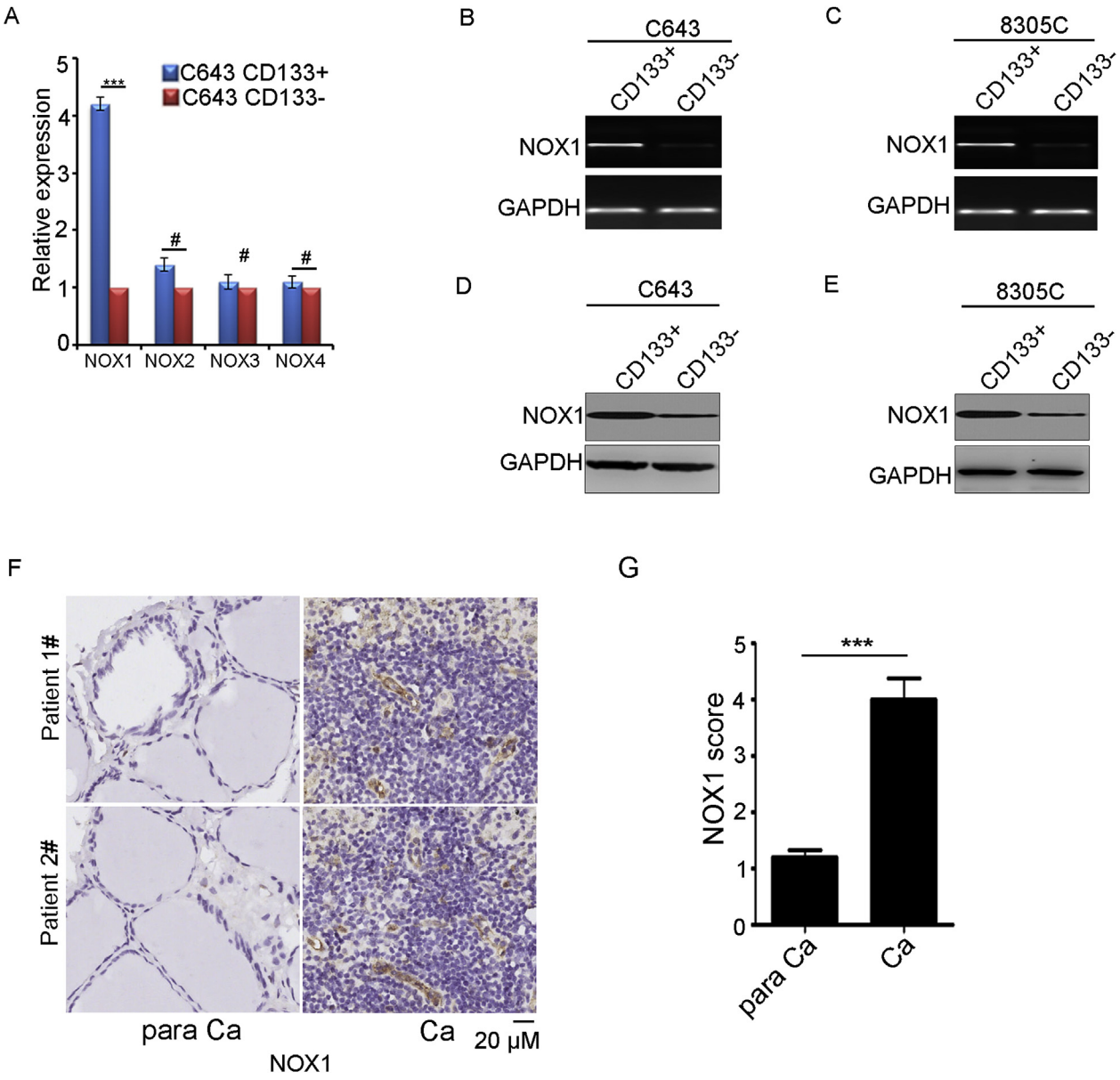

Fig. 2. NOX1 is highly expressed in CD133 + thyroid cancer cells. (A) QRT-PCR analysis was performed for NOX1-4 genes in CD133 + cells versus CD133- cells isolated from C643 xenograft. NOX members expression levels in CD133- cells were defined as 1 (calibrator), and the relative expression of each gene in CD133 + cells was expressed as the fold difference over CD133- cells. (B and C) RT-PCR analysis was performed for NOX1 in CD133 + cells versus CD133- cells isolated from C643 xenograft (B) or 8305C xenograft (C). GAPDH served as a loading control. (D and E) Western blot analysis was performed for NOX1 in CD133 + cells versus CD133- cells isolated from C643 xenograft (D) or 8305C xenograft (E). (F and G) (F) IHC staining for NOX1 in paired thyroid cancer tissues. Scale bar represents 20 μM. B. (G) The scores for quantitative staining of NOX1 in thyroid cancer tissues and para cancerous tissues were determined. Values are mean ± SEM; ***$p < 0.001$. Para Ca, para cancerous; Ca, cancer.

enhanced chemiluminescence substrate (Pierce Biotechnology). For quantification, the western blot films were scanned and were analyzed using ImageJ Version 1.33u software.

2.5. Quantitative RT-PCR

Total RNA was isolated with Trizol reagent (Invitrogen). cDNA was synthesized using the RT-PCR kit (TakaRA). Equal amounts of cDNA were mixed with Power SYBR Green PCR master mix (Applied Biosystems, Carlsbad, CA) and primers. GAPDH was amplified as an internal control. Experiments were performed using an ABI Prism 7500 System (Applied Biosystems). The relative quantification of each mRNA was calculated using the comparative Ct method. The crossing threshold value was noted for each transcript and normalized with the internal control. The sequences of primers used for PCR amplification are as follows: Sox2 (forward, 5′-AAATGGGAGGGGTGCAAAAGAG GAG-3′; reverse, 5′- CAGCTGTCATTTGCTGTGGGTGATG-3′); Nanog (forward, 5′- AATACCTCAGCCTCCAGCAGATG-3′; reverse, 5′- TGCGT CACACCATTGCTATTCTTC-3′); OCT4 (forward, 5′- CTTGCTGCAGAAG TGGGTGGAGGAA-3′; reverse, 5′- CTGCAGTGTGGGTTTCGGGCA-3′); GAPDH (forward, 5′-ACAACTTTGGTATCGTGGAAGG-3′; reverse, 5′-GCCATCACGCCACAGTTTC-3′); NOX1 (forward, 5′- CACAAGAAAA ATCCTTGGGTCAA -3′; reverse, 5′- GACAGCAGATTGCGACACACA -3′); NOX2 (forward, 5′- CAAGATGCGTGGAAACTACCTAAGAT -3′; reverse, 5′- TCCCTGCTCCCACTAACATCA-3′); NOX3 (forward, 5′- CCAGGGCA GTACATCTTGGT-3′; reverse, 5′—CCGTGT TTCCAGGGAGAGTA-3′); NOX4 (forward, 5′-TGGCTGCCCATCTGGTGAATG-3′; reverse, 5′- CAG CAGCCCTCCTGAAACATGC-3′).

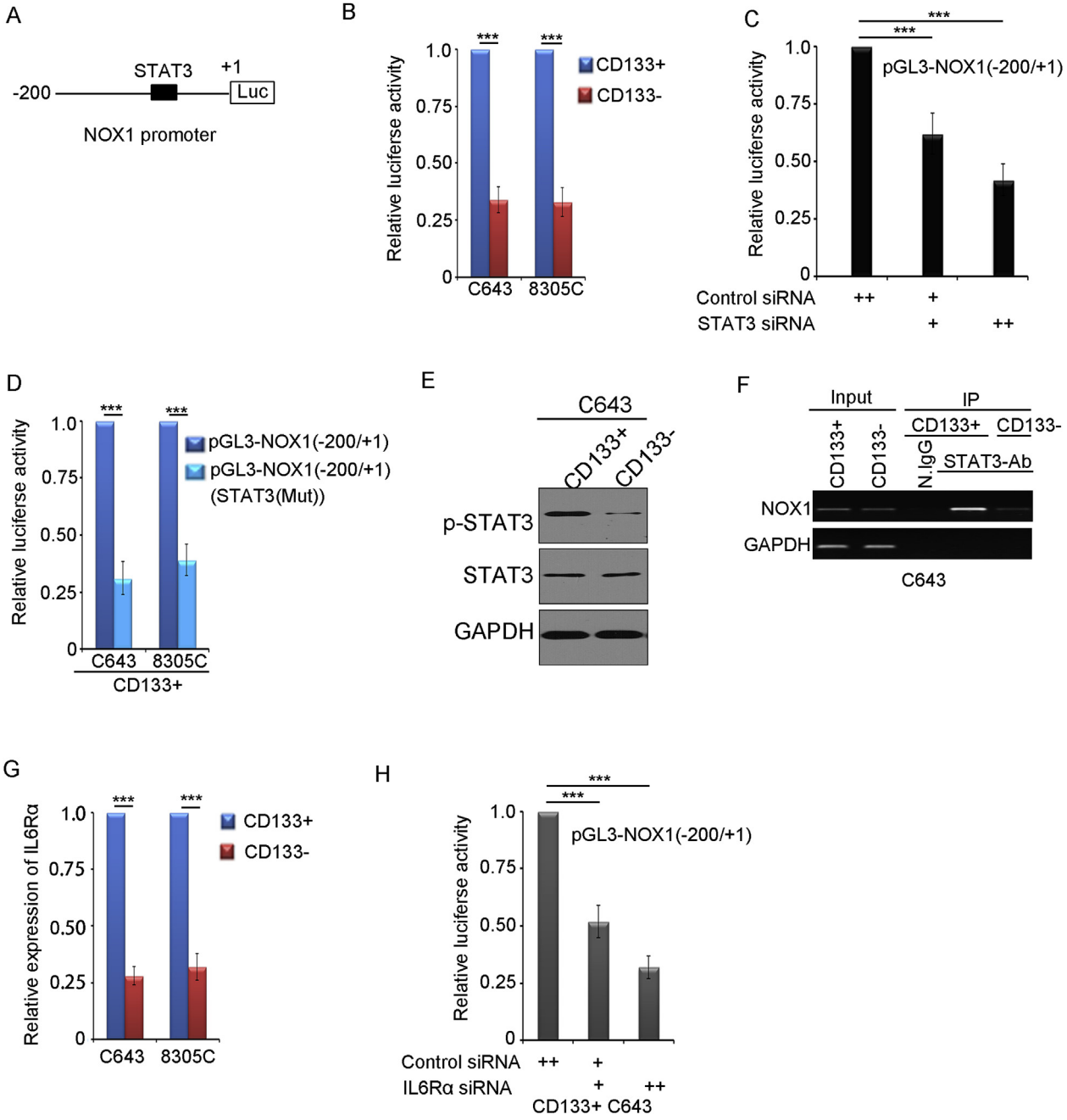

Fig. 3. Activation of STAT3 is responsible for up-regulation of the NOX1 expression in CD133 + thyroid cancer cells. (A) Schematic drawing of Nox1 promoters depicted the relative position of the STAT3-binding sites. (B) The NOX1 promoter construct pGL3-NOX1(-200/+1) was transiently co-transfected with pRL-SV40 into CD133 + cells or CD133- cells. The luciferase activity was determined. The values were presented as fold activation over CD133- cells. Values are mean ± SEM; ***$p < 0.001$. (C) The NOX1 promoter construct pGL3-NOX1(-200/+1) was transiently co-transfected with pRL-SV40 and control siRNA or STAT3 siRNA into CD133 + cells. The luciferase activity was determined. The values were presented as fold activation over CD133 + cells expressing control siRNA. Values are mean ± SEM; ***$p < 0.001$. (D) The NOX1 promoter construct pGL3-NOX1(-200/+1) or its mutant M(STAT3) was transiently co-transfected with pRL-SV40. The values were presented as fold activation over CD133 + cells expressing pGL3-NOX1(-200/+1). Values are mean ± SEM; ***$p < 0.001$. (E) Western blot analysis of STAT3 phosphorylation (Y705) level and total STAT3 level in CD133 + cells or CD133- cells. GAPDH served as a loading control. (F) ChIP assay of STAT3 binding to NOX1 promoter in CD133 + cells or CD133- cells. Immunoprecipitations were carried out with normal IgG (N.IgG), anti-STAT3 antibody (STAT3-Ab). Co-precipitating DNA was revealed by PCR with the indicated primers. Input DNA was diluted 50-fold before amplification. PCR primers for the NOX1 promoter or the GAPDH promoter were used to detect promoter fragments in immunoprecipitates. (G) QRT-PCR analysis was performed for IL-6Rα in CD133 + cells versus CD133- cells isolated from C643 xenograft or 8305C xenograft. CD133 + cells were defined as 1. Values are mean ± SEM; ***$p < 0.001$. (H) The NOX1 promoter construct pGL3-NOX1(-200/+1) was transiently co-transfected with pRL-SV40 and control siRNA or IL-6Rα siRNA into CD133 + cells. The luciferase activity was determined. The values were presented as fold activation over CD133 + cells expressing control siRNA. Values are mean ± SEM; ***$p < 0.001$.

2.6. Tumor formation assay

To examine the tumor-initiating capacity of CD133 + thyroid cancer cells or CD133- thyroid cancer cells, cells was transplanted into 6- to 8-week old immunodeficient mice in accordance with a Fudan University Institutional Animal Care and Use Committee approved protocol concurrent with national regulatory standards. Mice were sacrificed when they were moribund or 180 days after implantation.

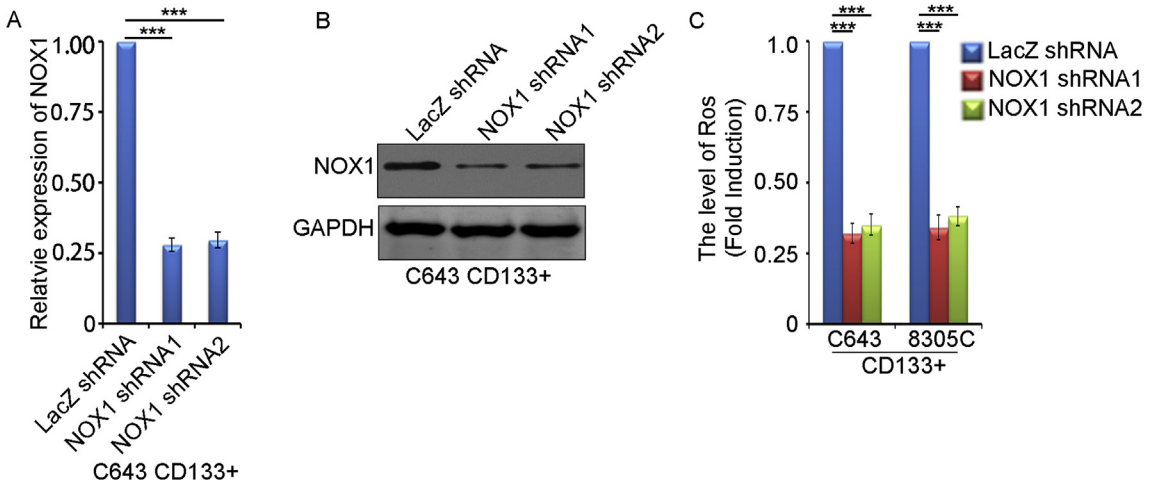

Fig. 4. High expression of NOX1 is responsible for the high ROS level in CD133 + thyroid cancer cells. (A) QRT-PCR analysis of NOX1 expression in CD133 + cells expressing LacZ shRNA or NOX1 shRNA. Values are mean ± SEM; ***$p < 0.001$. (B) Western blot analysis of NOX1 expression in CD133 + cells expressing LacZ shRNA or NOX1 shRNA. GAPDH expression served as a loading control. (C) The level of ROS in CD133 + cells isolated from C643 or 8305C xenograft expression LacZ shRNA or NOX1 shRNA were analyzed by FACS. ROS level in CD133 + cells were defined as 1. Results are expressed as mean ± SEM from three separate experiments; ***$p < 0.001$.

Tumor formation was determined by histology.

2.7. Detection of the intracellular redox state

Cells were incubated with 2 μM redox-sensitive probe, CM-H_2DCFDA (Molecular Probes) for 15 min of incubation at 37 °C. As the permeable positive control, 0.025% H_2O_2 was added 15 min prior to CM-H_2DCFDA. Oxidation of the probe was detected by the increase of FITC fluorescence. The true level of intracellular ROS was estimated by subtracting the background mean fluorescence intensity (MFI) of the non-fluorescent sample (negative control) from the measured MFI values of fluorescent samples in flow cytometry analysis. To examine the effect of NAC or BSO on the level of ROS, cells were pre-treated with NAC (sigma) or BSO (sigma) for 72 h.

2.8. Immunohistochemistry

Paraffin-embedded sections were deparaffinized and rehydrated. Antigens were retrieved by boiling sections in 10 mM sodium citrate (pH 6.0). After the endogenous peroxidase was blocked by incubating with 3% H_2O_2 solution in PBS for 10 min, sections were blocked with 5% normal serum and were incubated with primary antibody. After extensive washing in TBST, sections were incubated for 60 min with HRP-conjugated secondary antibody (Santa Cruz Biotechnology). The immunoreactivity was visualized with 3, 3-diaminobenzidine (Dako). The images were captured using the Motic Image Advanced 3.2 image analysis system. The scores for semi quantitative staining of the tissue sections (score 1–6) were determined according to a total score that was obtained by combining the score of the percentage of positive cells and the score of the staining intensity.

2.9. Statistical analysis

Results are expressed as the mean ± standard error of the mean (mean ± SEM). In general, significance was tested by unpaired two-tailed *Student's t*-test using GraphPad InStat 5.0 software. *P* values < 0.05 were considered statistically significant.

3. Results

3.1. The level of ROS is high in CD133 + thyroid cancer cells

CD133 is a marker of thyroid cancer stem cells [5]. We isolated CD133 + and CD133- cells from xenografts formed from thyroid cell lines C643 and 8305C. $CD133^+$ tumor cells displayed characteristics consistent with cancer stem cells: sphere formation (Fig. 1A); expression of stem cell markers (Fig. 1B and C); and high tumorigenicity in immunocompromised mice (Fig. 1D). Therefore, $CD133^+$ subpopulations are enriched for thyroid cancer stem cells.

Using this CD133-based selection system in conjunction with flow cytometry and the ROS-sensitive dye DCFDA, we compared ROS levels between CD133 + cells and CD133- cells. The level of ROS was higher in CD133 + cells than in CD133- cells isolated from xenografts formed from thyroid cancer cells (Fig. 1E; $p < 0.001$). These findings suggest that the level of ROS is high in CD133 + thyroid cancer cells.

3.2. ROS-generating oxidase NOX1 is highly expressed in CD133 + thyroid cancer cells

Endogenous ROS are mainly produced by NADPH oxidase (NOX) enzymes, which compose a family of seven enzymes, including NOX1-5 and DUOX1-2 [11,12]. We compared the expression of NOX members in CD133 + and CD133-thyroid cancer cells. Compared to matched CD133-cells, NOX1 mRNA expression was dramatically up-regulated in CD133 + cells (Fig. 2A). RT-PCR analysis confirmed this finding (Fig. 2B and C). We further compared NOX1 protein expression between CD133 + and CD133- thyroid cancer cells and found NOX1 protein level to be high in CD133 + cells (Fig. 2D and E). Next, we characterized NOX1 expressions during thyroid cancer progression. Compared to para tumor tissues, NOX1 was highly expressed in thyroid cancer tissues (Fig. 2F and G; $p < 0.001$). These findings suggest that NOX1 is highly expressed in CD133 + thyroid cancer cells.

3.3. Activation of STAT3 is responsible for up-regulation of the NOX1 expression in CD133 + thyroid cancer cells

To examine the mechanism of high NOX1 expression in CD133 + thyroid cancer cells, we generated the NOX1 reporter construct pGL3-NOX1(-200/+1), which retained relative strong promoter activity and contained one STAT3-binding site at nucleotides −80/-72

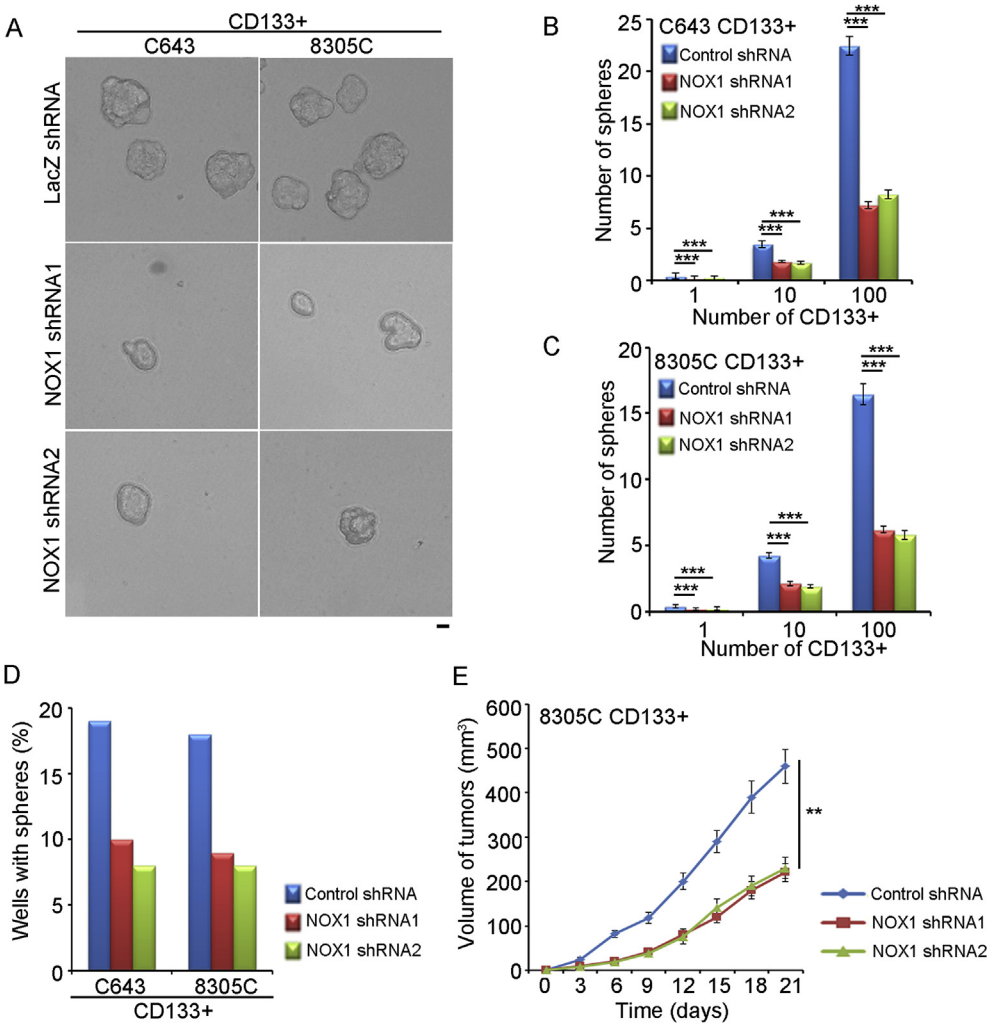

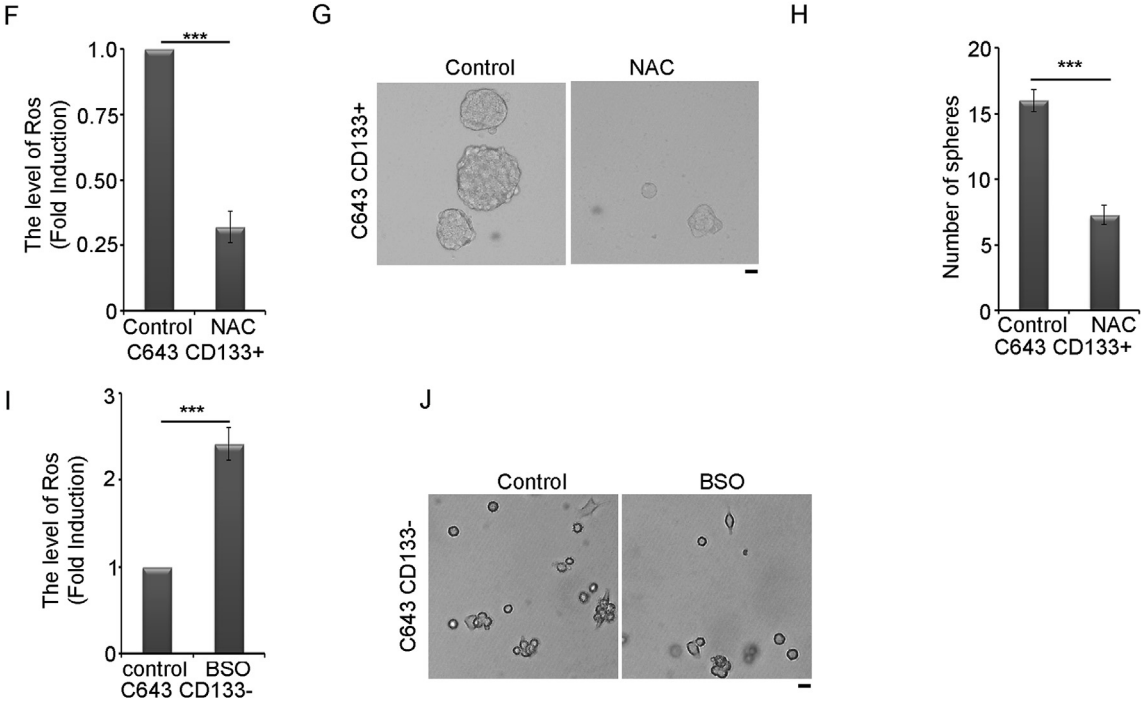

(caption on next page)

Fig. 5. NOX1 promotes the self-renewal ability of CD133 + thyroid cancer cells. (A) Single cell sphere formation assay of CD133 + cells expressing LacZ shRNA or NOX1 shRNA. Representative images of sphere are shown. Scale bar represents 20 μM. (B and C) A total of 1, 10, or 100 CD133 + cells isolated from C643 xenograft (B) or 8305C xenograft (C) expressing LacZ shRNA or NOX1 shRNA were cultured in 96-well plates. After 10 days, the number of sphere was counted. Results are expressed as mean ± SEM from three separate experiments; ***$p < 0.001$. (D) Secondary sphere formation assay of CD133 + cells expressing LacZ shRNA or NOX1 shRNA. Data mean the percentage of sphere containing wells in each group. (E) CD133 + cells from C643 xenograft expressing LacZ shRNA or NOX1 shRNA were subcutaneously implanted into immunocompromised mice. Tumor volumes were measured every 3 days after tumor cells inoculation. Results are expressed as mean ± SEM; **$p < 0.01$. (F) The level of ROS in CD133 + cells isolated from C643 xenograft treated with or without 5 mM NAC (N-acetylcysteine) for 72 h was analyzed by FACS. The level of ROS in CD133 + cells treated with control was defined as 1. Results are expressed as mean ± SEM from three separate experiments; ***$p < 0.001$. (G and H) 100 CD133 + cells isolated from C643 xenograft treated with or without 5 mM NAC (N-acetylcysteine) were cultured in 96-well plates. After 10 days, the number of sphere was counted. (G) Representative images of sphere are shown. Scale bar represents 20 μM. (H) Results are expressed as mean ± SEM from three separate experiments; ***$p < 0.001$. (I) The level of ROS in CD133-cells isolated from C643 xenograft treated with or without 10 μM BSO for 72 h were analyzed by FACS. The level of ROS in CD133- cells treated with control was defined as 1. Results are expressed as mean ± SEM from three separate experiments; ***$p < 0.001$. (J) 100 CD133- cells isolated from C643 xenograft treated with or without 10 μM BSO were cultured in 96-well plates for 10 days. Representative images of sphere are shown. Scale bar represents 10 μM.

(Fig. 3A) [13,14]. The NOX1 promoter activity was higher in CD133 + cells than in CD133- cells (Fig. 3B). We next examined the contribution of the activation of NOX1 promoter by STAT3 to NOX1 high expression in CD133 + cells. Down-regulation of STAT3 using siRNA obviously reduced activation of the NOX1 promoter (Fig. 3C). The STAT3-binding site was then modified using site-directed mutagenesis to create M(STAT3), which reduced NOX1 promoter activity in CD133+ thyroid cancer cells (Fig. 3D). STAT3 becomes activated upon phosphorylation at Tyr705, which induces dimerization, nuclear translocation, and DNA binding [15,16]. We next compared STAT3 phosphorylation levels in CD133 + and CD133- cells and found high levels of STAT3 Y705 phosphorylation in CD133 + cells (Fig. 3E). Consistent with this, CHIP assay revealed more binding of STAT3 to the NOX1 promoter in CD133 + cells than in CD133- cells (Fig. 3F). STAT3 is usually activated by the IL-6/IL-6Rα signaling pathway [17,18], and IL-6Rα is highly expressed in cancer stem cells [19]. Analysis using qRT-PCR revealed that IL-6 Rα was more highly expressed in CD133 + cells (Fig. 3G). Furthermore, down-regulation of IL-6Rα reduced NOX1 promoter activity (Fig. 3H). Together, these data indicates that induction of STAT3 phosphorylation is responsible for high activation of the NOX1 promoter in CD133 + thyroid cancer cells.

3.4. High expression of NOX1 is responsible for the high ROS levels in CD133 + thyroid cancer cells

The contribution of high NOX1 expression to high ROS levels observed in CD133 + cells was examined using a lentiviral shRNA-based system targeting NOX1 expression. Knockdown of NOX1 in CD133 + cells significantly reduced NOX1 mRNA levels and protein levels (Fig. 4A and B). Furthermore, knockdown of NOX1 clearly reduced ROS levels in CD133 + cells isolated from C643 xenografts and 8305C xenografts (Fig. 4C). These data indicates that high NOX1 expression is responsible for the high ROS levels observed in CD133 + thyroid cancer cells.

3.5. NOX1 promotes the self-renewal activity of CD133 + thyroid cancer cells

The contribution of NOX1 to CD133 + thyroid cancer cells self-renewal activity and tumorigenicity was examined using a lentiviral shRNA-based system targeting NOX1 expression. Sphere formation assay is the conventional method of measuring the self-renewal capacity of cancer stem cells [20,21]. NOX1 knockdown impaired sphere formation not only in primary assays (Fig. 5A–C), but also in secondary passages (Fig. 5D), indicating the requirement of NOX1 for CD133 + thyroid cancer cells self-renewal in vitro. Furthermore, NOX1 knockdown reduced the growth rate of CD133 + thyroid cancer cells in vivo (Fig. 5E). Third, we examined the effect of altered ROS levels on the self-renewal activity of CD133 + thyroid cancer cells. BSO (L-buthionine sulfoximine), an inhibitor of glutathione (GSH) synthesis, and NAC (N-acetyl-L-cysteine), a widely-used antioxidant against ROS, were used to endogenously increase and decrease, respectively, intracellular ROS levels [22,23]. NAC reduced the level of ROS (Fig. 5F), and inhibited the sphere formation ability of CD133 + cells (Fig. 5G and H). Although BSO increased the level of ROS (Fig. 5I), BSO did not promote the sphere formation of CD133- cells (Fig. 5J). Together, NOX1 promotes the self-renewal property of CD133 + thyroid cancer cells.

3.6. NOX1 promotes the self-renewal property of CD133 + thyroid cancer cells through activation of the Akt signaling

ROS activates the PI3K/Akt pathway through the reversible inactivation of the PTEN protein [24]. PI3K/Akt pathway maintains the self-renewal ability of cancer stem cells [25]. The contribution of Akt pathway to NOX1 promoting CD133 + thyroid cancer cells self-renewal was examined. Analysis using PI3K enzyme-linked immunosorbent assay revealed that NOX1 knock down significantly reduced PI3K activity in CD133 + cells (Fig. 6A). NOX1 knock down clearly reduced Akt phosphorylation without obvious changes of the total Akt level (Fig. 6B and C). Furthermore, overexpression of a constitutively active form of Akt rescued the negative effect of NOX1 knockdown on the self-renewal capability of CD133 + thyroid cancer cells. (Fig. 6D and E). Together, NOX1 promotes the self-renewal activity of CD133 + thyroid cancer cells through activation of the Akt signaling.

4. Discussion

In this study, we found that the level of ROS was higher in CD133 + thyroid cancer cells than in CD133- thyroid cancer cells. High expression of ROS-generating oxidase NOX1 induced by STAT3 activation was responsible for the high ROS level in CD133 + thyroid cancer cells. NOX1 promoted the self-renewal property of CD133 + thyroid cancer cells partly through activation of the Akt signaling (Fig. 6F). These results suggest that ROS are necessary for CD133 + thyroid cancer cells self-renewal.

Normal and cancer Stem cells generally have been thought to maintain low levels of ROS as a protection against DNA damage. In breast tumor, CSCs contain lower ROS levels than corresponding non-tumorigenic cells [26]. Higher ROS levels limit hematopoietic stem cells their lifespan [27]. In thyroid cancer, ROS-low cells are more spherogenic than ROS-high cells [23]. In contrast to these studies, ROS generated by Nox1 are necessary for spermatogonial stem cells self-renewal in vitro [28]. In proliferative neural stem cells, high levels of ROS promote self-renewal by driving PI3K/AKT signaling [29]. In colorectal cancer, ROS facilitates Wnt-driven intestinal SC proliferation leading to colorectal cancer [30]. In airway basal stem cells, moderate ROS levels activate Nrf2, which activates the Notch pathway to stimulate airway basal stem cells self-renewal [31]. Together, the role of ROS in normal and cancer stem cells maintenance appears to be context and tissue specific. Low ROS levels protect stem cells from DNA damage; moderate ROS levels stimulate stem cell self-renewal. In this

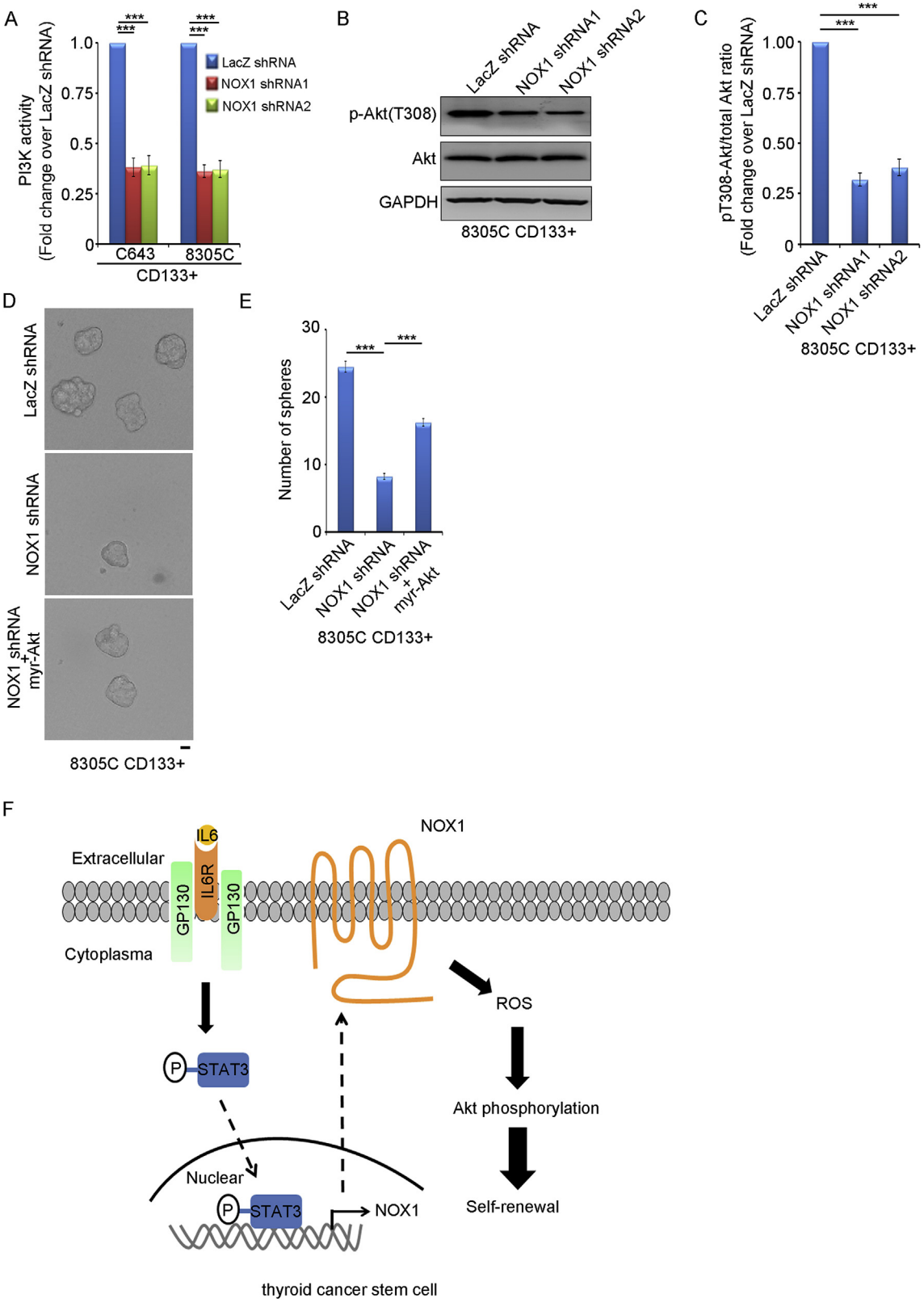

Fig. 6. NOX1 promotes the self-renewal property of CD133 + thyroid cancer cells through activation of the Akt signaling. (A) The PI3K activity of CD133 + cells expressing LacZ shRNA or NOX1 shRNA were assessed using a PI3 kinase ELISA kit. Values are normalized to that of CD133 + cells expressing LacZ shRNA. Results are expressed as mean ± SEM from three separate experiments; ***$p < 0.001$. (B and C) (B) Western blot analysis of Akt T308 phosphorylation level and Akt total level in CD133 + cells expressing LacZ shRNA or NOX1 shRNA. GAPDH expression served as a loading control. (C) The relative densities of pT308-Akt to total Akt in B were quantified using densitometry. Values are normalized to that of CD133 + cells expressing LacZ shRNA. Results are expressed as mean ± SEM from three separate experiments; ***$p < 0.001$. (D and E) A total of 100 CD133 + cells isolated from C643 xenograft expressing LacZ shRNA or NOX1 shRNA or/and myr-Akt (active form of Akt) were cultured in 96-well plates for 10 days. (D) Representative images of sphere are shown. Scale bar represents 20 μM. (E) The number of sphere was counted. Results are expressed as mean ± SEM from three separate experiments; ***$p < 0.001$. (F) Schematic modeling of STAT3-activated NOX1 expression and downstream signaling activities, promoting the self-renewal ability of CD133 + thyroid cancer cells.

present study, our data suggest that ROS promotes the self-renewal ability of CD133 + thyroid cancer cells. In accordance with this, CD133 + clonal SW620 cells displayed high tumorigenesis ability and higher cellular reactive oxygen species (ROS) [32]. We would hypothesize that increased ROS facilitates CD133 + thyroid cancer cells self-renewal during thyroid cancer progression.

The cellular ROS are majorly generated by NOX family members (NOXs 1–5, DUOX1, and DUOX2) [33,34]. We found that NOX1 mRNA expression was higher in CD133 + thyroid cancer cell than in CD133- cells. Knock down of NOX1 reduced ROS level in CD133 + thyroid cancer cells. STAT3 binds to NOX1 promoter and induces NOX1 promoter activity [13]. CHIP assay revealed that the binding of STAT3 to NOX1 promoter was higher in CD133 + cells than in CD133- cells. The activity of STAT3 phosphorylation was higher in CD133 + cells than in CD133- cells. Together, high expression of NOX1 induced by STAT3 activation was responsible for the high ROS level in CD133 + thyroid cancer cells. STAT3 is an important regulator of cancer stem cells self-renewal [35]. Our findings might provide a new mechanism of STAT3 regulating cancer stem cells self-renewal.

Increasing evidence suggests the functional association of CD133 + cancer stem cells with Akt signaling. CD133 + tumor cells derived from hepatoma, colon cancer, neuroblastoma and glioma consistently displayed increased phospho-Akt levels compared with matched CD133- tumor cells [36–39]. In glioma, the interaction between CD133 and p85 activates Akt phosphorylation in CD133 + glioma stem cells [39]. In neuroblastoma, high expression of neurotrophic receptor activates Akt phosphorylation in CD133 + neuroblastoma cells [40]. In this present study, our data reveal that high expression of NOX1 in CD133 + thyroid cancer cell activates Akt phosphorylation. Our finding might provide a new mechanism of Akt activation in CD133 + cancer stem cells.

In conclusion, ROS-generating oxidase NOX1 promotes the self-renewal property of CD133 + thyroid cancer cells at least partly through activation of the Akt signaling. These findings provide a new mechanism sustaining the self-renewal of thyroid cancer stem cells.

Conflicts of interest

Authors have no conflicts of interests.

Author contributions

CW performed most experiments; ZLW performed cells sorting; ZLW, WL, and ZLA helped animal experiments; ZLA discussed the data and wrote the manuscript.

Funding

This work was supported by National Natural Science Foundation of China. (81272722).

Acknowledgements

We are grateful to Dr. Jing Li (Shanghai Medical College of Fudan University) for providing flow cytometry technology.

Appendix A. Supplementary data

Supplementary data to this article can be found online at https://doi.org/10.1016/j.canlet.2019.01.028.

References

[1] R. Vigneri, P. Malandrino, P. Vigneri, The changing epidemiology of thyroid cancer: why is incidence increasing? Curr. Opin. Oncol. 27 (2015) 1–7.
[2] E.Y. Ibrahim, N.L. Busaidy, Treatment and surveillance of advanced, metastatic iodine-resistant differentiated thyroid cancer, Curr. Opin. Oncol. 29 (2017) 151–158.
[3] Z. Yao, L. Mishra, Cancer stem cells and hepatocellular carcinoma, Cancer Biol. Ther. 8 (2009) 1691–1698.
[4] J. Zhou, Y. Zhang, Preclinical development of cancer stem cell drugs, Expert Opin. Drug Discov. 4 (2009) 741–752.
[5] R.Y. Lin, Thyroid cancer stem cells, Nat. Rev. Endocrinol. 7 (2011) 609–616.
[6] W. Zhu, T. Hai, L. Ye, G.J. Cote, Medullary thyroid carcinoma cell lines contain a self-renewing CD133+ population that is dependent on ret proto-oncogene activity, J. Clin. Endocrinol. Metab. 95 (2010) 439–444.
[7] S. Prasad, S.C. Gupta, A.K. Tyagi, Reactive oxygen species (ROS) and cancer: role of antioxidative nutraceuticals, Cancer Lett. 387 (2017) 95–105.
[8] L. Tong, C.C. Chuang, S. Wu, L. Zuo, Reactive oxygen species in redox cancer therapy, Cancer Lett. 367 (2015) 18–25.
[9] M. Ushio-Fukai, Y. Nakamura, Reactive oxygen species and angiogenesis: NADPH oxidase as target for cancer therapy, Cancer Lett. 266 (2008) 37–52.
[10] V. Nogueira, N. Hay, Molecular pathways: reactive oxygen species homeostasis in cancer cells and implications for cancer therapy, Clin. Canc. Res. 19 (2013) 4309–4314.
[11] B. Pinegin, N. Vorobjeva, M. Pashenkov, B. Chernyak, The role of mitochondrial ROS in antibacterial immunity, J. Cell. Physiol. 233 (2018) 3745–3754.
[12] A.K. Jayavelu, J.N. Moloney, F.D. Bohmer, T.G. Cotter, NOX-driven ROS formation in cell transformation of FLT3-ITD-positive AML, Exp. Hematol. 44 (2016) 1113–1122.
[13] A. Manea, L.I. Tanase, M. Raicu, M. Simionescu, Jak/STAT signaling pathway regulates nox1 and nox4-based NADPH oxidase in human aortic smooth muscle cells, Arterioscler. Thromb. Vasc. Biol. 30 (2010) 105–112.
[14] H.K. Lee, D.W. Park, J.H. Bae, H.J. Kim, D.G. Shin, J.S. Park, et al., RGS2 is a negative regulator of STAT3-mediated Nox1 expression, Cell. Signal. 24 (2012) 803–809.
[15] J. Bosch-Barrera, B. Queralt, J.A. Menendez, Targeting STAT3 with silibinin to improve cancer therapeutics, Cancer Treat Rev. 58 (2017) 61–69.
[16] J. Huynh, N. Etemadi, F. Hollande, M. Ernst, M. Buchert, The JAK/STAT3 axis: a comprehensive drug target for solid malignancies, Semin. Canc. Biol. 45 (2017) 13–22.
[17] M. Zhao, Y. Tan, Q. Peng, C. Huang, Y. Guo, G. Liang, et al., IL-6/STAT3 pathway induced deficiency of RFX1 contributes to Th17-dependent autoimmune diseases via epigenetic regulation, Nat. Commun. 9 (2018) 583.
[18] H. Zhang, Y. Song, H. Yang, Z. Liu, L. Gao, X. Liang, et al., Tumor cell-intrinsic Tim-3 promotes liver cancer via NF-kappaB/IL-6/STAT3 axis, Oncogene 37 (2018) 2456–2468.
[19] H. Wang, J.D. Lathia, Q. Wu, J. Wang, Z. Li, J.M. Heddleston, et al., Targeting interleukin 6 signaling suppresses glioma stem cell survival and tumor growth, Stem Cell. 27 (2009) 2393–2404.
[20] Z. Guo, H. Hardin, R.V. Lloyd, Cancer stem-like cells and thyroid cancer, Endocr. Relat. Cancer 21 (2014) T285–T300.
[21] Y. Wang, X. Lin, X. Fu, W. Yan, F. Lin, P. Kuang, et al., Long non-coding RNA BANCR regulates cancer stem cell markers in papillary thyroid cancer via the RAF/MEK/ERK signaling pathway, Oncol. Rep. 40 (2018) 859–866.
[22] C.H. Chiang, C.H. Chuang, S.L. Liu, C.F. Chian, H. Zhang, J.H. Ryu, N-acetylcysteine attenuates ventilator-induced lung injury in an isolated and perfused rat lung model, Injury 43 (2012) 1257–1263.
[23] M. Shimamura, K. Yamamoto, T. Kurashige, Y. Nagayama, Intracellular redox status controls spherogenicity, an in vitro cancer stem cell marker, in thyroid cancer cell lines, Exp. Cell Res. 370 (2018) 699–707.
[24] M.A. Chetram, A.S. Don-Salu-Hewage, C.V. Hinton, ROS enhances CXCR4-mediated functions through inactivation of PTEN in prostate cancer cells, Biochem. Biophys. Res. Commun. 410 (2011) 195–200.
[25] S. Singh, J. Trevino, N. Bora-Singhal, D. Coppola, E. Haura, S. Altiok, et al., EGFR/Src/Akt signaling modulates Sox2 expression and self-renewal of stem-like side-population cells in non-small cell lung cancer, Mol. Canc. 11 (2012) 73.
[26] M. Diehn, R.W. Cho, N.A. Lobo, T. Kalisky, M.J. Dorie, A.N. Kulp, et al., Association of reactive oxygen species levels and radioresistance in cancer stem cells, Nature 458 (2009) 780–783.
[27] K. Ito, A. Hirao, F. Arai, K. Takubo, S. Matsuoka, K. Miyamoto, et al., Reactive oxygen species act through p38 MAPK to limit the lifespan of hematopoietic stem cells, Nat. Med. 12 (2006) 446–451.
[28] H. Morimoto, K. Iwata, N. Ogonuki, K. Inoue, O. Atsuo, M. Kanatsu-Shinohara, et al., ROS are required for mouse spermatogonial stem cell self-renewal, Cell Stem Cell 12 (2013) 774–786.
[29] J.E. Le Belle, N.M. Orozco, A.A. Paucar, J.P. Saxe, J. Mottahedeh, A.D. Pyle, et al., Proliferative neural stem cells have high endogenous ROS levels that regulate self-renewal and neurogenesis in a PI3K/Akt-dependant manner, Cell Stem Cell 8 (2011) 59–71.
[30] K.B. Myant, P. Cammareri, E.J. McGhee, R.A. Ridgway, D.J. Huels, J.B. Cordero, et al., ROS production and NF-kappaB activation triggered by RAC1 facilitate WNT-driven intestinal stem cell proliferation and colorectal cancer initiation, Cell Stem Cell 12 (2013) 761–773.
[31] M.K. Paul, B. Bisht, D.O. Darmawan, R. Chiou, V.L. Ha, W.D. Wallace, et al., Dynamic changes in intracellular ROS levels regulate airway basal stem cell homeostasis through Nrf2-dependent Notch signaling, Cell Stem Cell 15 (2014) 199–214.
[32] J.M. Feng, Z.H. Miao, Y. Jiang, Y. Chen, J.X. Li, L.J. Tong, et al., Characterization of the conversion between CD133+ and CD133- cells in colon cancer SW620 cell line, Cancer Biol. Ther. 13 (2012) 1396–1406.
[33] G.J. Maghzal, K.H. Krause, R. Stocker, V. Jaquet, Detection of reactive oxygen

species derived from the family of NOX NADPH oxidases, Free Radic. Biol. Med. 53 (2012) 1903–1918.
[34] R.M. Touyz, A.M. Briones, M. Sedeek, D. Burger, A.C. Montezano, NOX isoforms and reactive oxygen species in vascular health, Mol. Interv. 11 (2011) 27–35.
[35] L.L. Marotta, V. Almendro, A. Marusyk, M. Shipitsin, J. Schemme, S.R. Walker, et al., The JAK2/STAT3 signaling pathway is required for growth of CD44(+)CD24(-) stem cell-like breast cancer cells in human tumors, J. Clin. Invest. 121 (2011) 2723–2735.
[36] S. Ma, T.K. Lee, B.J. Zheng, K.W. Chan, X.Y. Guan, CD133+ HCC cancer stem cells confer chemoresistance by preferential expression of the Akt/PKB survival pathway, Oncogene 27 (2008) 1749–1758.
[37] H. Sartelet, T. Imbriglio, C. Nyalendo, E. Haddad, B. Annabi, M. Duval, et al., CD133 expression is associated with poor outcome in neuroblastoma via chemoresistance mediated by the AKT pathway, Histopathology 60 (2012) 1144–1155.
[38] Y.K. Wang, Y.L. Zhu, F.M. Qiu, T. Zhang, Z.G. Chen, S. Zheng, et al., Activation of Akt and MAPK pathways enhances the tumorigenicity of CD133+ primary colon cancer cells, Carcinogenesis 31 (2010) 1376–1380.
[39] Y. Wei, Y. Jiang, F. Zou, Y. Liu, S. Wang, N. Xu, et al., Activation of PI3K/Akt pathway by CD133-p85 interaction promotes tumorigenic capacity of glioma stem cells, Proc. Natl. Acad. Sci. U.S.A. 110 (2013) 6829–6834.
[40] H. Takenobu, O. Shimozato, T. Nakamura, H. Ochiai, Y. Yamaguchi, M. Ohira, et al., CD133 suppresses neuroblastoma cell differentiation via signal pathway modification, Oncogene 30 (2011) 97–105.